

Electronic Structure, Local Moments and Transport in Fe_2VAl

D.J. Singh

Code 6691, Naval Research Laboratory, Washington, DC 20375

I.I. Mazin

Code 6691, Naval Research Laboratory, Washington, DC 20375 and CSI, George

Mason University, Fairfax, VA 22030

(October 6, 2018)

Abstract

Local spin density approximation calculations are used to elucidate electronic and magnetic properties of Heusler structure Fe_2VAl . The compound is found to be a low carrier density semimetal. The Fermi surface has small hole pockets derived from a triply degenerate Fe derived state at Γ compensated by an V derived electron pocket at the X point. The ideal compound is found to be stable against ferromagnetism. Fe impurities on V sites, however, behave as local moments. Because of the separation of the hole and electron pockets the RKKY interaction between such local moments should be rapidly oscillating on the scale of its decay, leading to the likelihood of spin-glass behavior for moderate concentrations of Fe on V sites. These features are discussed in relation to experimental observations of an unusual insulating state in this compound.

A. Introduction

The physics of metal insulator transitions, although much better understood now than a few years ago, continues to attract interest, especially in proximity to unusual magnetic

behavior or where odd transport properties are observed on the metallic or insulating sides of the transition.

Nishino et al.^{1,2} recently reported a highly unusual insulating state in Heusler phase $(\text{Fe}_{1-x}\text{V}_x)_3\text{Al}$ alloys at $x = 1/3$. At this composition, the Fe and V are believed to separate on the two transition metal sub-lattices, yielding a well ordered compound. The resistivity decreases smoothly from the lowest measured temperature of 2 K to over 1200 K, characteristic of an insulator. However, the dependence is clearly non-exponential and has a finite low temperature value of approximately 3 m Ω ·cm. This unusual resistivity is accompanied by the presence of a clear Fermi edge in photoemission spectra and a large finite linear component of the specific heat, $\gamma = 14$ mJ/mol·K². It was noted that plots of specific heat over temperature, C/T vs. T^2 show an upturn with decreasing temperature, reminiscent of heavy fermion systems, perhaps related to spin-fluctuations.

Compositions with slightly less V (lower x) have metallic resistivities at low temperature, and order magnetically, while higher V concentration samples display more normal semiconducting behavior. The ordering is plainly ferromagnetic at low $x \lesssim 0.2$ and presumably so up to $x = 1/3$. The Curie temperature, T_C decreases monotonically to zero with increasing x from almost 800 K at $x = 0$ reaching room temperature near $x = 0.2$. In this ferromagnetic regime, the resistivity as a function of temperature is metallic though with generally high low temperature saturation values, has a maximum at T_C and then crosses over to a decreasing T dependence, somewhat like the colossal magnetoresistive manganites. The prominence of this cross-over feature increases rapidly with decreasing T_C . There is no evidence for magnetic ordering at $x = 1/3$ or higher. However, based on the temperature of the resistivity maximum as a function of composition, Fe_2VAl is at or very close to the composition where T_C reaches zero, again suggestive of strong spin fluctuations.

$(\text{Fe}_{1-x}\text{V}_x)_3\text{Al}$ alloys occur in a Heusler DO_3 structure throughout the composition and temperature range of interest. This structure is derived from a simple cubic B2 (CsCl) structure, FeAl , by replacing every second Al by a transition metal atom in an fcc way. Thus it has a single Al site and two inequivalent transition metal sites in the four atom unit cell.

The first transition metal site, denoted Fe1, accommodates one atom, and is coordinated by eight transition metal atoms on the other type of site. The second, Fe2, accommodates two atoms and is coordinated by 4 Al and four Fe1 transition metal atoms. It is important to note that the Fe1 site is quite different from the Fe2 site, both in terms of coordination and size. Particularly, the Fe1 site is larger and has no Al neighbors. Not unexpectedly, V, being larger, prefers to occupy Fe1 site^{2,3} leading to the L2₁ ordered compound Fe₂VAl. This is reflected in the sharp upturn in lattice parameter as a function of composition at $x = 1/3$, where the Fe1 site becomes completely V filled, resulting in occupation of the Fe2 site with the larger V species. Nonetheless, Fe₂VAl is hardly a narrow line compound, and there could well be significant Fe occupation of the nominal V, Fe1 sites in as measured $x = 0.33$ samples.

In this paper, we report electronic structure studies of the (Fe_{1-x}V)₃Al system focussing on the $x = 1/3$ composition, in order to create a framework for understanding its properties. These local spin density approximation (LSDA) calculations show fully ordered Fe₂VAl to be a semimetal, with separated electron and hole pockets and a very low carrier density. This is of some interest in itself, since it is a situation favorable for exciton formation. Remarkably, the compound is not near a ferromagnetic instability, and in fact has a low spin susceptibility, related to the low carrier density. However, we find that Fe atoms on the nominal V, Fe1 site display strong local moment magnetism. The transport and other anomalous properties are discussed in terms of the band structure and the interactions with the dilute Fe1 local moment system.

B. Approach

All atoms in the fcc DO₃ and ordered L2₁ crystal structure occur on high symmetry sites. Accordingly, the only free crystallographic parameter is the lattice parameter. The LSDA calculations presented here are based on the reported¹ experimental lattice parameter of 0.576 nm. The electronic structure provides the underlying basis for our discussion

of transport properties, and accordingly we wished to obtain it as accurately as possible. The band structures, densities of states and fixed spin moment calculations were all done using the general potential linearized augmented planewave method⁴, including local orbital extensions to relax linearization errors, and well converged basis sets of over 350 functions for the four atom unit cells.⁵ LAPW spheres of radius 2.30 a.u. were employed for all sites.

The high site symmetries (the lowest symmetry site is the Fe2, which is tetrahedral) and bcc-like close packing, suggest that linear muffin tin orbital atomic sphere approximation (LMTO-ASA) calculations may also be reasonably reliable. We have performed parallel calculations using the Stuttgart *TB LMTO-4.7* code^{6,7} to test this. We find that, apart from small band shifts, the two codes yield identical results. Thus we were able to use the LMTO method to study the local changes that occur for transition metal defects in Fe₂VAl. This was done using a series of LMTO supercell calculations. In particular we modeled defects in which Fe atoms were placed on V sites in various magnetic and structural configurations, in order to establish their magnetic character and interactions. We used *spd* orbitals for all atoms, plus downfolded *f* states on Fe for the LMTO calculations.

C. Electronic structure of ordered stoichiometric Fe₂VAl.

The LSDA band structure of ordered Fe₂VAl is shown in Fig. 1. The corresponding electronic density of states (DOS) and projections onto LAPW spheres is shown in Fig. 2. Before discussing the details near the Fermi energy, E_F , that relate to the transport properties, we overview the basic structure. No magnetic instability was found for this composition, and as such the bands are non-spin-polarized. The 3 eV wide split-off band at the bottom that disperses upwards from Γ derives from the Al 3*s* state. The remainder of the valence band manifold, which extends from approximately -6 eV to $+2$ eV may be described as 15 transition metal 3*d* derived bands, with three Al 3*p* derived bands dispersing through. However, due to a Fano-type mixing with the transition metal bands, the Al free electron-like character is depleted in the main transition metal region and piles up at the

top ($2 - 3$ eV, relative to E_F) and bottom ($-6 - -5$ eV) of the manifold.

There is a strong pseudogap around E_F . The states above the gap are generally of mixed V and Fe e_g character, while those below are for the most-part more Fe-like.

The separation of the V d states into two well-separated peaks in the DOS is mainly due to crystal field. With the bcc like coordination of the V site, its d manifold is split into a lower lying set of three t_{2g} states, around -2 eV, relative to E_F , and two e_g states around $+1$ eV. For the Fe d bands the effects of hybridization are stronger than the crystal field. This Fe-Fe hybridization involves primarily Al and V states, although direct hopping is also substantial (the Fe - Fe distance is $a/2$: not much longer than the Fe-V and Fe-Al distances of $a\sqrt{3}/4$). Based on down-folding of the LMTO band structure, and the positions of the bands at Γ , we estimate the Fe crystal field splitting to be quite small, of the order of 0.35 eV, apparently due to canceling contributions from the tetrahedral coordinations with V and Al atoms. In any case, as may be seen from the positions and characters of the bands at Γ , the ordering of Fe d sub-levels from lowest to highest is e_g bonding, t_{2g} bonding, t_{2g} anti-bonding and e_g anti-bonding. Of these, all but the e_g anti-bonding states are below the pseudogap.

However, the pseudogap is not complete because the top of the Fe anti-bonding t_{2g} band, which occurs at the Γ point, is above the bottom of the V e_g band. The reason is that V $dd\sigma$ hopping is comparatively large, and that in an fcc lattice (the V sublattice in Fe_2VAl is fcc) the lower e_g band is often strongly (by $1.5 t_{dd\sigma}$) dispersive along $\Gamma\text{-}\mathbf{X}$ direction, so the bottom of this V-derived band (at the \mathbf{X} point) occurs below the top of the anti-bonding Fe t_{2g} band (at the Γ point)

Fig.3 shows a blow-up of the band structure near E_F . There are four bands crossing E_F . These contribute three small hole pocket sheets of Fermi surface centered at Γ , compensated by a larger electron like Fermi surface section centered at the X point of the fcc Brillouin zone. The occupation is 0.012 electrons/f.u. (2.5×10^{20} el./cm³), compensated by an equal number of holes. The Γ centered surfaces derive from the Fe t_{2g} bands with a small admixture of V character. The electron pocket at X is purely V e_g (there is no Fe d character at the

X point by symmetry). The Γ hole surfaces consist of three pockets with the effective mass $m \approx 0.5 m_e$; however, the surfaces deviate noticeably from the sphere, due to the finite, albeit small, band filling, and the effective masses at the Fermi level vary from $0.35 m_e$ to $1 m_e$. The X centered electron sections are ellipsoids with the effective masses $m_x = 0.55 m_e$ and $m_y = 0.25 m_e$. The low carrier density corresponds to a low density of states, $N(E_F) = 0.3 \text{ eV}^{-1}$ with a bare specific heat coefficient, $\gamma_{\text{bare}} = 0.65 \text{ mJ/mol}\cdot\text{K}^2$. Comparing with the experimental value, this yields a large enhancement of more than 20, certainly not characteristic of a simple metal.

Two candidate mechanisms for yielding such behavior are strong spin-fluctuations and strong electron-electron correlations. With regard to the latter, it is noteworthy that the band structure near E_F consists of small separated electron and hole sections with low carrier density, and that there are manifolds of flat transition metal d bands in close proximity both above and below the pseudogap. The formation of bound electron-hole pairs (excitons) leading to a correlated insulating state in zero gap semiconductors and semimetals was much discussed in the 1970's.⁸ Qualitatively, the formation of such a state in semimetals is possible when certain conditions are met. These are (a) low enough carrier density for the pairs not to overlap; (b) exciton binding energy larger than the distance from the band edge to E_F (if scattering is significant, or a more complicated criterion related to nesting of the hole and electron sections if the mean free path is long⁹); and (c) mean free path long compared to the exciton radius. Given the experimental data, particularly indications of spin fluctuations (which would scatter carriers), the high residual resistivities, and smooth behavior as a function of x , it seems unlikely that these conditions are met in Fe_2VAl .

The low carrier density implies that a simple Stoner instability of the non-spin-polarized state, due to divergence of the susceptibility $\chi(q)$, will not occur, since the $N(E_F)$ factor will be too small. However, the absence of an instability against small fluctuations does not necessarily mean that a magnetic state with larger moments is not present. A local moment system on the verge of ordering is consistent with many of the experimental observations and would have strong spin fluctuations that could yield the size of enhancements observed.

Fixed spin moment calculations were used to address this possibility. The energy as a function of magnetization, shown in Fig.4, provides no evidence of any interesting magnetic behavior in ordered stoichiometric Fe_2VAl . In particular, the energy is a smooth monotonically increasing function of magnetization. After a very small parabolic region extending to approximately $0.02 \mu_B/\text{f.u.}$, the curve becomes roughly linear up to $2.5 \mu_B/\text{f.u.}$, and then crosses over to an upward curving form. The linear region is due to the semi-metallic character of the material. As the bands are split by the exchange enhanced applied field in the fixed spin moment calculation, $N(E_F)$ increases from a low value. This leads to a corresponding increase in the differential susceptibility, flattening the curve from parabolic. The induced moments are almost entirely associated with the Fe sub-lattice in Fe_2VAl . Up to $4 \mu_B/\text{f.u.}$, the V site contributes a small ($\sim 5\%$ of the total) negative contribution, while by $5 \mu_B/\text{f.u.}$, the V contribution becomes parallel to the Fe, but is still very small.

D. Magnetic Properties of Defects

This begs the question of the magnetic properties of defects, since some explanation of the magnetic properties is needed. As mentioned, when all the V on the Fe1 site is replaced by Fe, i.e. in Fe_3Al , the material is strongly ferromagnetic. As V is put back in (entering the larger Fe1 site), ferromagnetism is gradually suppressed, disappearing just at the point where the Fe1 site is fully substituted with V. On the other hand, the above fixed spin moment calculations indicate that V is magnetically inactive on the Fe1 site. One may then conjecture that magnetism is coming from the Fe atoms on the Fe1 site. Although little is known about defects in Fe_2VAl , if it follows the pattern of other compound aluminides, defects in which the small atom (Fe) sits on the larger sites (Al and V), either accompanied by non-stoichiometry or compensating vacancies are likely. There are some experimental indications¹⁰ that this is indeed the case in $\text{Fe}_{2+x}\text{V}_{1-x}\text{Al}$. Given the variation of lattice parameter with composition, showing a sharp increase at $x = 1/3$ and the wide range of V/Fe compositions that can be made, we conjecture that Fe atoms on the nominally V, Fe1

site may be a common defect in the experimentally studied samples.

To study the behavior of such defects, we performed a series of supercell calculations for various $\text{Fe}_{2+x}\text{V}_{1-x}\text{Al}$ compounds, using the LMTO-ASA method. Most of the supercells were produced by doubling or quadrupling the unit cell along the (111) direction, resulting in a rhombohedral symmetry. A convenient nomenclature for such supercells is obtained by listing the sequence of the [111] planes. For this type of supercell, the crystallography of the Heusler structure is such that, given a sequence of the [111] planes $\cdots\text{ABCDEFG}\cdots$, the atom D has 3 nearest neighbors (n.n.) of the kind C, 3 n.n. of the kind E, 1 n.n. of the kind A, and 1 of the kind G (but no n.n. in planes B or F), as illustrated in Fig. 5. Thus, such a notation lets one immediately see the environment of each atom (recall that every atom sits in the center of a cube formed by its 8 n.n. as in the B2, CsCl structure).

To start with, let us look at the stoichiometric compound Fe_2VAl , but placing V on one of the Fe2 sites, and one of the Fe's on the Fe1 site. This results in the following sequence:

$$\cdots \text{V}|\text{Fe}'\text{Al}\underline{\text{FeFeV}}\text{AlFe}''\text{V}|\text{Fe}'\cdots, \quad (1)$$

where the underlined atoms have been interchanged. We find a ferromagnetic ordered state with the moments inside the atomic spheres $2.1 \mu_B$ on $\underline{\text{Fe}}$, $1.1 \mu_B$ on Fe'' , $0.6 \mu_B$ on Fe' , and $-0.2 \mu_B$ on V (note the minus sign, in accord with the fixed-moment LAPW calculations). All other atoms carry negligible moments. This is to be compared with the moments in pure Fe_3Al in LMTO-ASA calculations, which are $2.3 \mu_B$ for Fe1 and $1.8 \mu_B$ for Fe2; see also Ref.¹¹ (LAPW calculations yield 2.4 and $1.9 \mu_B$, respectively). Fe on Fe1 sites that are magnetically active and in turn polarize Fe2 Fe atoms. Magnetic moments on Fe1, but not on Fe2, are essentially local moments: they hardly depends on the Fe1's environment or electron count as is illustrated by the other supercell calculations, described below. Fe' and Fe'' in (1) have the same n.n. environment, but different next n.n. environments. Correspondingly, the induced magnetization, totaling $1.8 \mu_B$ per 2 atoms, is unevenly distributed between Fe' and Fe'' . In real samples one expects that V on Fe2 site, if any, may occupy all Fe2 sites randomly. To investigate this, we repeated the above calculations with a virtual crystal of

the structure

$$\dots V|\mathcal{M}''\text{Al}\mathcal{M}'\underline{\text{Fe}}\mathcal{M}'\text{Al}\mathcal{M}''V|\mathcal{M}''\dots, \quad (2)$$

where \mathcal{M} has atomic number $Z = 25.25$ ($\text{V}_{0.25}\text{Fe}_{0.75}$), still isoelectronic with Fe_2VAl .

The moment on $\underline{\text{Fe}}$ was again $2.1 \mu_B$, that on \mathcal{M}'' was $0.75 \mu_B$, and on \mathcal{M}' it was $0.15 \mu_B$. In other words, although now the moment was equally distributed between the two \mathcal{M}'' atoms, the total magnetization induced in this sublattice changed very little. An interesting question is why \mathcal{M}' atoms, which have among n.n. three strongly polarized Fe atoms, are not magnetic, while the \mathcal{M}'' atoms, having only one spin-polarized n.n., are.

It is instructive to see how Fe on Fe1 sites behaves in more Fe-rich compounds, particularly, how defects in which V is placed into a smaller Fe2 site (as in the above-considered supercells) influence the magnetic properties? To answer this question, we prepared supercells with nominal stoichiometries, $\text{Fe}_{2.5}\text{V}_{0.5}\text{Al}$ and $\text{Fe}_{2.25}\text{V}_{0.75}\text{Al}$. The former was, in the above notation,

$$\dots V|\text{Fe}''\text{AlFe}'\underline{\text{Fe}}\text{Fe}'\text{AlFe}''V|\text{Fe}''\dots, \quad (3)$$

while the latter was a quadrupled fcc cell and retaining full cubic symmetry. In the former case we obtain $M = 2.4 \mu_B$ on $\underline{\text{Fe}}$ (very slightly larger than in Fe_3Al) and $0.7 \mu_B$ on Fe'' , in accord with the virtual crystal calculation described above. The $\text{Fe}_{2.25}\text{V}_{0.75}\text{Al}$ compound produced $2.2 \mu_B$ on $\underline{\text{Fe}}$ with no significant polarization on the other sites.

Taken together, these calculations indicate that Fe on a Fe1 site acquires strong, localized magnetic moment of 2.2–2.3 μ_B , which is robust against redistribution of Fe and V atoms within the transition metal sublattices and even changes in the total V concentration. As a further test we performed supercell calculations with a further doubling of the unit cell (3) of $\text{Fe}_{2.5}\text{V}_{0.5}\text{Al}$ and performed calculations with antiferromagnetic ordering:

$$\dots (\text{Fe}''\text{AlFe}'\underline{\text{Fe}}\text{Fe}'\text{AlFe}''V)[\text{Fe}''\text{AlFe}'\underline{\text{Fe}}\text{Fe}'\text{AlFe}''V]\dots. \quad (4)$$

We found a metastable antiferromagnetic self-consistent solution with $\underline{\text{Fe}}$ having $\pm 2.3 \mu_B$ and Fe'' having $\pm 0.6 \mu_B$. That is, the moment on $\underline{\text{Fe}}$ was virtually the same as in the ferromagnetic

case, and that on Fe'' was only slightly suppressed. It seems that, independent of the spin arrangement of other Fe atoms, Fe on Fe1 site has enough room to act like a quasi-free ion, with the crystal splitting larger than the e_g and t_{2g} subband widths, and thus is unavoidably magnetic. Fe on the Fe2 site, on the other hand, is squeezed by larger Al and V ions and has subband widths large compared to their splitting. Thus it is intrinsically nonmagnetic, although moments can be induced on this site. In fact, in all supercell calculations, the partial DOS on Fe has two clear maxima, corresponding to the e_g and t_{2g} subbands (as in the non-spin-polarized case), while the DOS on the other Fe atoms shows relatively structureless broad bands.

E. Discussion

The above calculations show two main features. First of all Fe₂VAI is semi-metallic with a low carrier density and well separated hole and electron Fermi surface sections. Secondly, defects in which Fe atoms occur on the nominally V Fe1 sites provide local moments. Although this in itself does not provide an explanation of the anomalous properties, we speculate that the odd properties of this system may be due to the dynamics of a dilute system of such local moments and their interaction with the charge carriers.

An interesting point, worth mentioning, is that the direct exchange interaction of the localized Fe1 moments should be very small. One may then ask if there is an oscillating RKKY type interaction that could lead to a spin glass state in the same manner as in classical spin glass systems. The fact that the Fermi surfaces are small does not mean that the period of the RKKY interaction in this system is very long of the order of $2\pi/k_F$; rather, it is controlled by the wave vector connecting the hole and electron Fermi surfaces, which is π/a . That is, the relevant scale is set not by the size of the Fermi surfaces, but their separation. In fact, the RKKY interaction in this system can be written as

$$H_{RKKY}(\mathbf{r}) \approx 6H_{RKKY}^0(\mathbf{r})(\cos x/a + \cos y/a + \cos z/a), \quad (5)$$

where $H_{RKKY}^0(\mathbf{r})$ is the standard RKKY interaction¹², a function of k_F and effective mass

and the factor 3 appears because of degeneracy of the hole Fermi surfaces. $H_{RKKY}^0(\mathbf{r})$ changes with \mathbf{r} as $\cos(k_F r)$, where $k_F \approx 0.1\pi/a$, and thus is a long wavelength modulation. The RKKY interaction has a prefactor proportional to k_F^4 ; one effect of the smallness of the Fermi surfaces is that the interaction will be fairly weak compared with the traditional metallic RKKY spin glasses. Nevertheless, spin-glass effects cannot be excluded and it is tempting to ascribe the increase of the resistivity at $T \rightarrow 0$, and anomalously large specific heat coefficient γ , to a spin glass transition with a freezing temperature close to zero. It is worth noting that the temperature dependence γ is also unusual, with a large negative T^2 term. In this scenario, the properties will be sensitive to the ordering and concentration of local moments, i.e. Fe on the Fe1 site. Presumably this will be reflected in a high sensitivity to the exact composition and growth conditions. In this picture the magnetic properties of Fe rich alloys near $x = 1/3$ are then those of a local moment system with concentration increasing as x is reduced.

F. Acknowledgments

Computations were performed using facilities of the DoD HPCMO ASC Center. Work at the Naval Research Laboratory is supported by the Office of the Naval Research.

REFERENCES

- ¹ Y. Nishino, M. Kato, S. Asano, K. Soda, M. Hayasaki, and U. Mizutani, Phys. Rev. Lett. **79**, 1909 (1997).
- ² Y. Nishino, C. Kumada, and S. Asano, Scr. Mater. **36**, 461 (1997).
- ³ D.E. Okpalugo, J.G. Booth and C.A. Faunce, J. Phys. **F 15**, 681 (1985).
- ⁴ D.J. Singh, *Planewaves, Pseudopotentials and the LAPW Method*, Kluwer, Boston (1994).
- ⁵ D. Singh, Phys. Rev. **B43**, 6388 (1991).
- ⁶ O.K. Andersen, Phys. Rev. **B12**, 3060 (1975); O.K. Andersen and O. Jepsen, Phys. Rev. Lett. **53**, 2571 (1984).
- ⁷ O.K. Andersen and O. Jepsen, Phys. Rev. Lett., **53**, 2571 (1984).
- ⁸ B.I. Halperin and T.M. Rice, Rev. Mod. Phys. **40**, 755 (1968); D. Sherington and W. Kohn, *ibid*, 767 (1968); A.A. Abrikosov and S.D. Beneslavskii, J. Low Temp. Phys. **5**, 141 (1971).
- ⁹ Yu. V. Kopaev and T.T. Mnatsakanov, Fiz. Tverd. Tela **15**, 744 (1973) [Sov. Phys. Sol. State **16**, 520 (1973)].
- ¹⁰ E. Popiel, M. Tuszynski, W. Zarek and T. Rendecki, J. Less Common Met. **146**, 127 (1989).
- ¹¹ S.K. Bose, V. Drchal, J. Kudrnovsky, O. Jepsen, and O.K. Andersen, Phys. Rev. **B55**, 8184 (1997).
- ¹² C. Kittel, *Quantum Theory of Solids*, Wiley & Sons, NY, 1966.

FIGURES

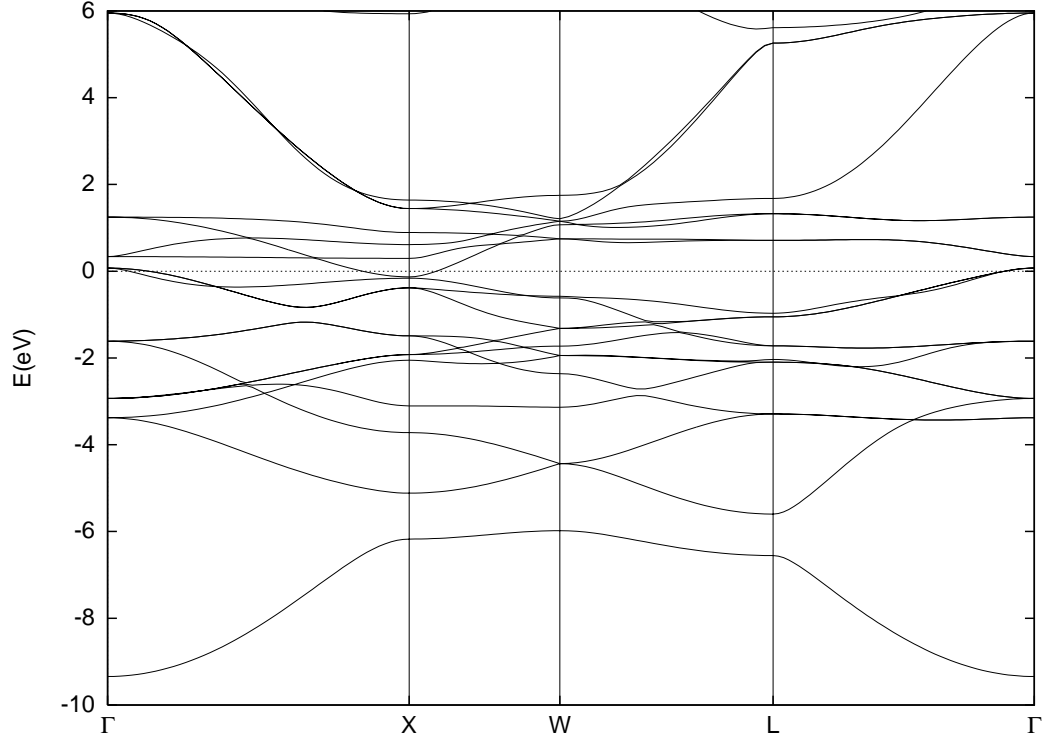


FIG. 1. Calculated band structure of Fe₂VAl. The Fermi energy is denoted by the dashed horizontal line at 0.

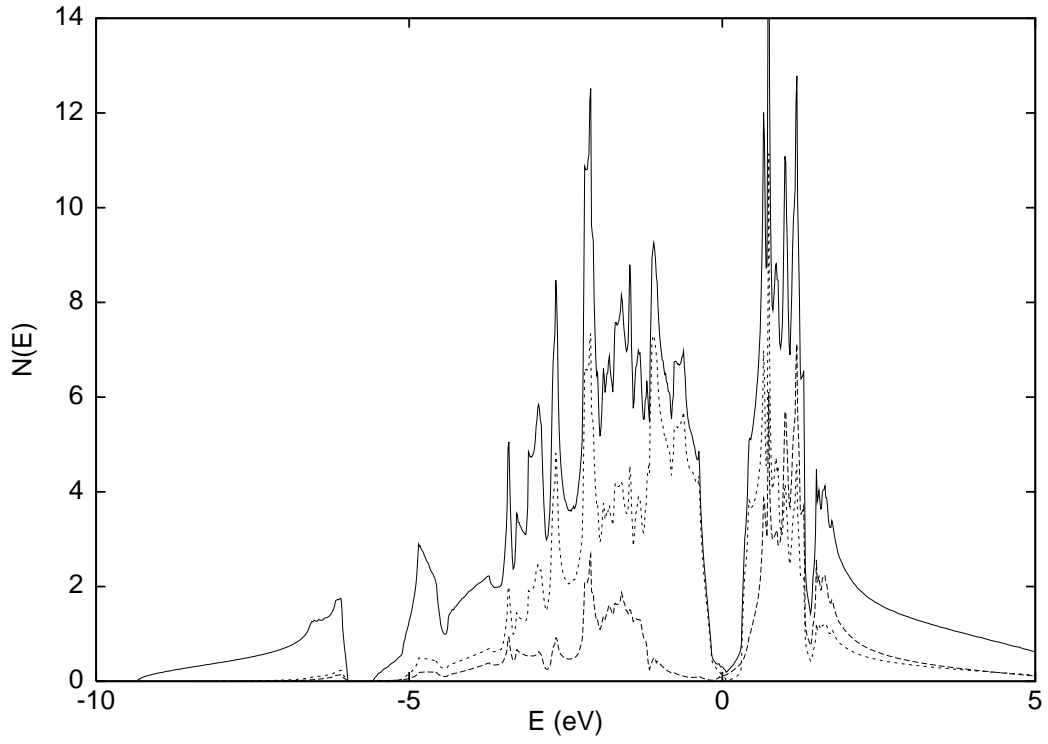


FIG. 2. Total and projected DOS of Fe_2VAl on a per formula unit basis. The total DOS is given by the solid line, while Fe d and V d contributions defined by the projections onto LAPW spheres are given by the dotted and dashed lines, respectively. The Fermi energy is at 0.

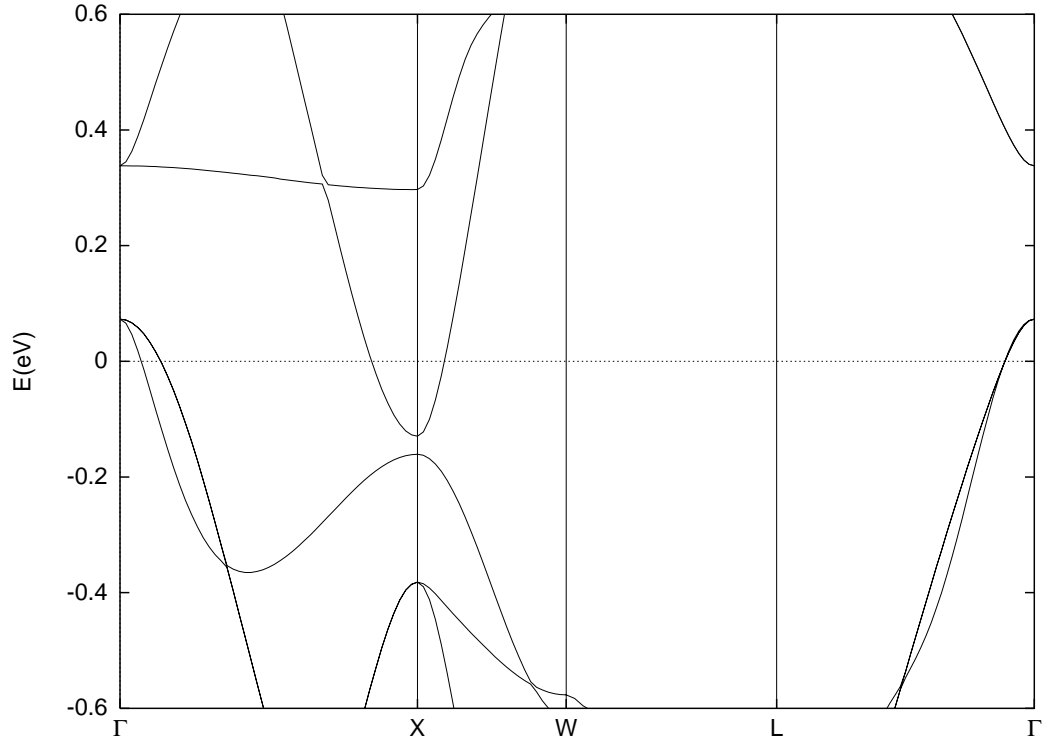


FIG. 3. Blowup of the band structure of Fe₂VAl near E_F .

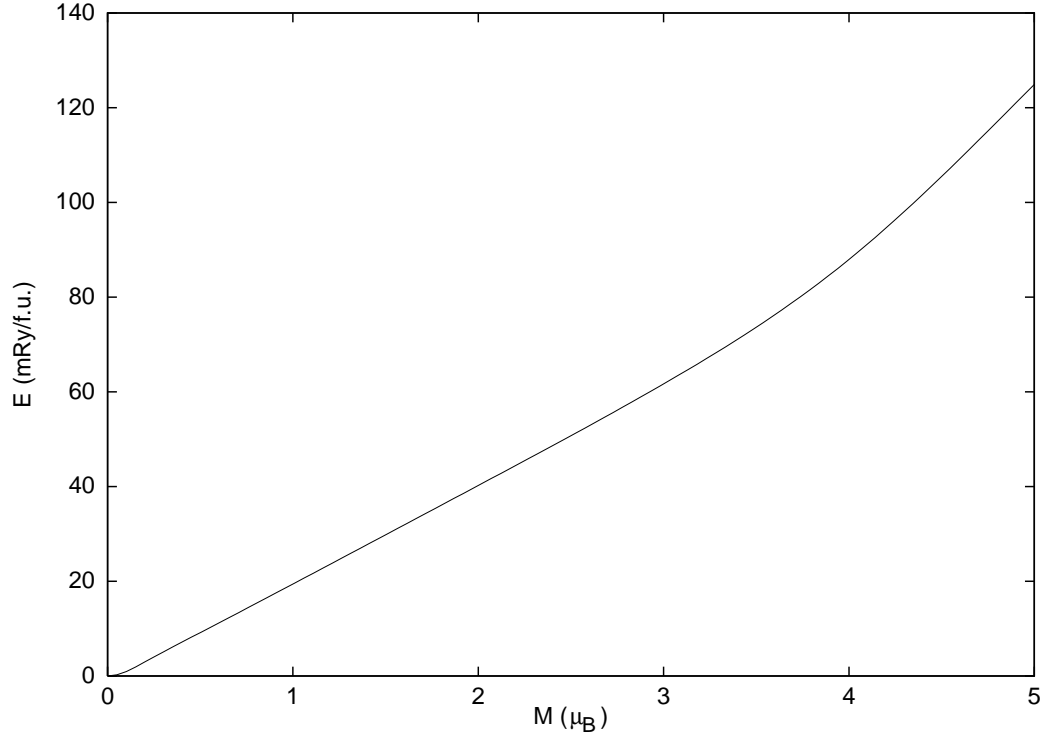


FIG. 4. Energy vs. imposed magnetization from fixed spin moment calculations for stoichiometric Fe_2VAl on a per formula unit basis.

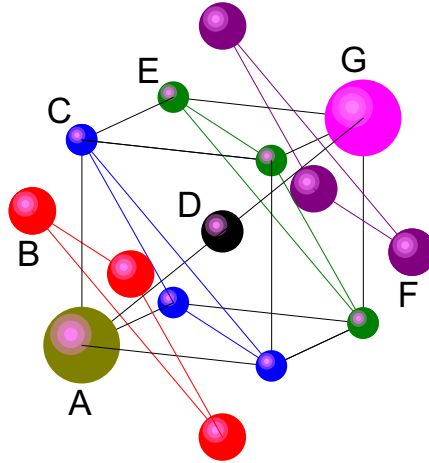


FIG. 5. Illustration of the coordination in Heusler type lattices, labeled as in the supercell calculations (see text).